Cell Reports

Report

OLFM4 regulates the antimicrobial and DNA binding activity of neutrophil cationic proteins

Graphical abstract

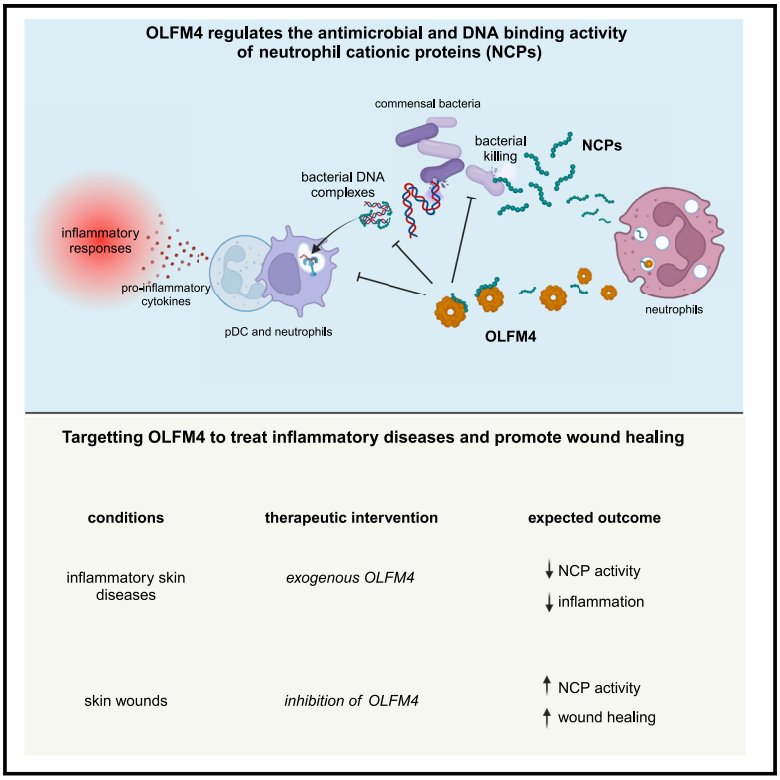

Highlights

- OLFM4 is a negatively charged protein that interferes with NCP oligomerization
- OLFM4 inhibits neutrophil-mediated bacterial killing
- OLFM4 inhibits TLR9 activation by NCP-DNA complexes in pDCs and neutrophils
- OLFM4 inhibition accelerates skin wound closure

Authors

Sophie Vandenberghe-Dürr, Michel Gilliet, Jeremy Di Domizio

Correspondence

michel.gilliet@chuv.ch (M.G.), jeremy.di-domizio@chuv.ch (J.D.D.)

In brief

Neutrophil cationic proteins (NCPs) have antibacterial, pro-inflammatory, and tissue repair properties. Vandenberghe-Dürr et al. show that OLFM4, a negatively charged granule molecule, disrupts NCP functions, impairing bacterial clearance and skin wound repair. Inhibiting OLFM4 therefore represents an attractive therapeutic strategy to accelerate skin wound closure.

Vandenberghe-Dürr et al., 2024, Cell Reports *43*, 114863
October 22, 2024
https://doi.org/10.1016/j.celrep.2024.114863

CellPress

Cell Reports

CellPress
OPEN ACCESS

Report

OLFM4 regulates the antimicrobial and DNA binding activity of neutrophil cationic proteins

Sophie Vandenberghe-Dürr,[1] Michel Gilliet,[1,*] and Jeremy Di Domizio[1,2,*]
[1]Department of Dermatology and Venereology, University Hospital of Lausanne UNIL-CHUV, 1011 Lausanne, Switzerland
[2]Lead contact
*Correspondence: michel.gilliet@chuv.ch (M.G.), jeremy.di-domizio@chuv.ch (J.D.D.)
https://doi.org/10.1016/j.celrep.2024.114863

SUMMARY

Neutrophil cationic proteins (NCPs) are a group of granule antimicrobial and inflammatory proteins released by activated neutrophils. These proteins primarily function via their positively charged structure, which facilitates interactions with bacterial membranes and the formation of immunogenic DNA complexes, thereby contributing to the initiation of wound repair in injured skin. After analyzing the structural properties of secreted neutrophil granule proteins, we identified OLFM4 as the only negatively charged molecule that interferes with NCP oligomerization. Through this interference, OLFM4 can inhibit neutrophil-mediated bacterial killing and DNA complex-dependent activation of Toll-like receptor 9 (TLR9) in plasmacytoid dendritic cells (pDCs) and neutrophils. While addition of exogenous OLFM4 blocks these processes, OLFM4 inhibition enhances neutrophil-dependent bacterial killing and DNA complex formation, ultimately leading to accelerated closure of skin wounds.

INTRODUCTION

Neutrophils play a pivotal role in antimicrobial and inflammatory responses by migrating to sites of tissue injury or infection and releasing neutrophil cationic proteins (NCPs). NCPs are positively charged proteins that can interact with and disrupt bacterial membranes through insertion into phospholipid bilayers.[1–3] One well-known NCP is LL-37, a small antimicrobial peptide derived from the cathelicidin protein.[4] Other examples are α-defensins (human neutrophil peptide 1 [HNP-1] and HNP-3),[5] lysozyme (LYZ),[6] and lactoferrin (LTF),[6,7] which all have antimicrobial activity against a wide range of pathogens.

During bacterial lysis, certain NCPs can also bind nucleic acids, forming immunogenic DNA complexes.[1–3] These complexes facilitate the delivery of DNA into immune cell compartments, triggering activation of endosomal TLR9 and cytosolic cyclic GMP-AMP synthase (cGAS)-stimulator of interferon genes (STING).[2,8] Besides bacterial DNA, NCPs can also interact with host-derived self-DNA released by dying host cells and neutrophil extracellular traps (NET)-forming neutrophils.[9,10] In such cases, NCPs may promote pro-inflammatory responses to remove damaged host cells and facilitate tissue repair. For instance, in skin wounds, complexes between NCPs and commensal bacterial DNA activate plasmacytoid dendritic cells (pDCs) and accelerate wound closure by inducing type I interferon (IFN) secretion[11,12].

However, excessive formation of NCP-DNA complexes may drive inflammatory diseases. In conditions like pustular psoriasis, these complexes activate neutrophils to secrete interleukin-1 (IL-1) cytokines and chemokines that sustain the pathogenic autoinflammatory response.[13] Additionally, the overexpression of NCPs and the formation of excessive self-DNA complexes have been linked to the development of inflammatory conditions such as plaque-type psoriasis,[14–16] lupus,[10,17] autoimmune diabetes,[18] and atherosclerosis.[19] These observations emphasize the need for tight control of NCP activity to avoid excessive inflammatory responses that contribute to disease development.

Olfactomedin 4 (OLFM4) is an OLFM domain-containing glycoprotein that is expressed by gut epithelial cells and is stored in secondary granules of neutrophils.[20,21] OLFM4 reduces antibacterial responses; in fact, elevated OLFM4 levels are linked to exacerbated human malaria infection[22] and poorer outcome of septic patients[23,24] Conversely, mice deficient for OLFM4 are protected against *Escherichia coli* and *Staphylococcus aureus* infection[25,26] as well as *H. pylori* gastric colonization,[27] suggesting a control of antimicrobial responses by OLFM4. A link between OLFM4 and the control of inflammatory responses is suggested by the finding that OLFM4 may inhibit NOD1 and NOD2-mediated nuclear factor κB (NF-κB) activation in gastric mucous cells.[27] However, the precise mechanism underlying OLFM4's ability to dampen antimicrobial and inflammatory responses remains poorly understood.

Here, we found that OLFM4 is a key player in dampening neutrophil-dependent antimicrobial and inflammatory responses. This occurs by binding to NCPs and neutralizing their ability to kill bacteria and form immunogenic complexes with DNA. Remarkably, when OLFM4 is neutralized, these processes

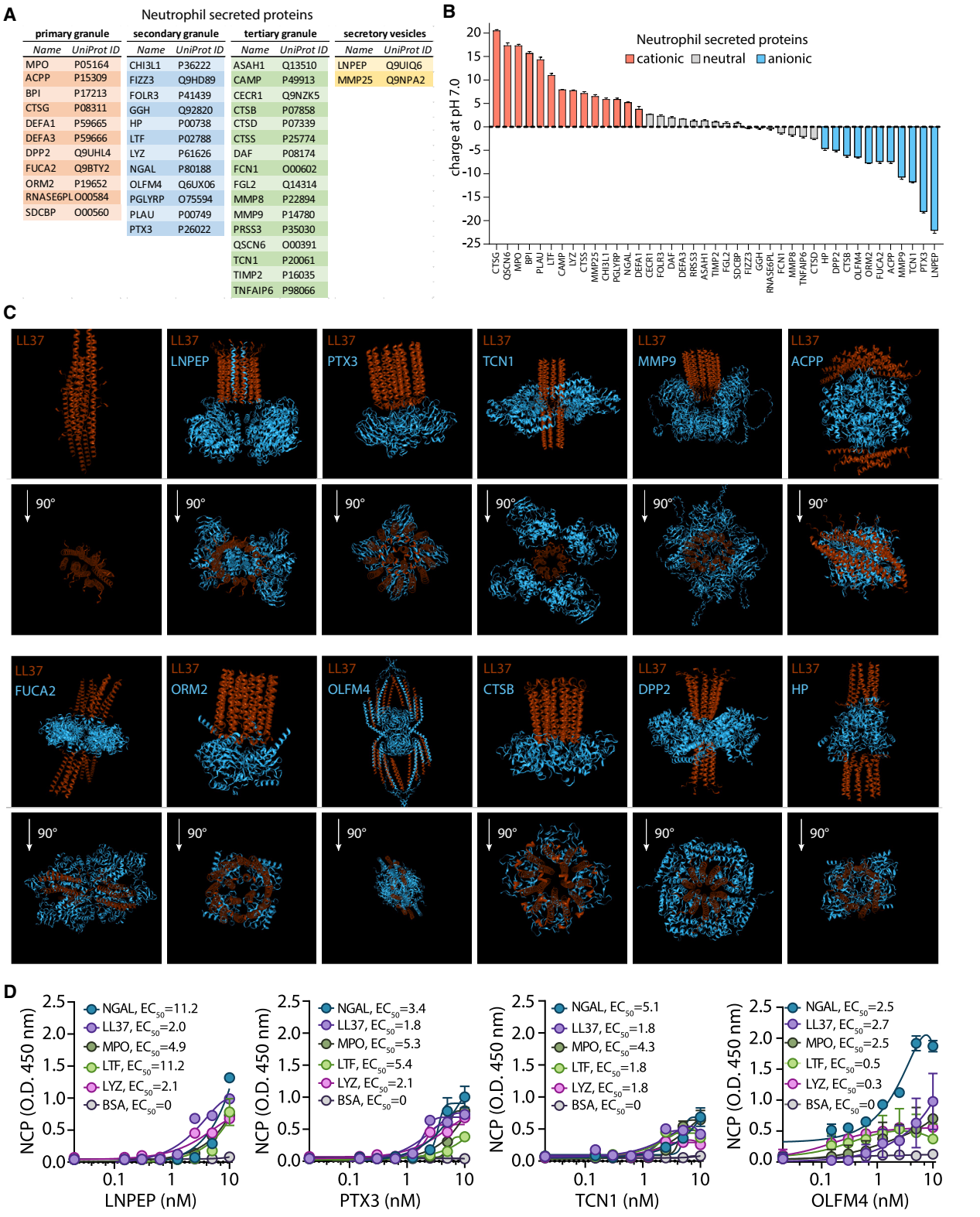

Figure 1. Neutrophils release negatively charged molecules that can bind multiple cationic proteins

(A) List of the most abundant granule proteins secreted by neutrophils. The name and UniProt ID of each protein are given.

(B) Net charge of the secreted neutrophil granule proteins at pH 7.0, calculated with 9 different acid dissociation constant (pKa) scales.

(legend continued on next page)

are enhanced, resulting in accelerated wound healing of injured skin. Our data highlight OLFM4 as a key regulatory factor in balancing neutrophil-dependent antimicrobial and inflammatory responses and uncover a new therapeutic target to promote wound healing.

RESULTS

Neutrophils release negatively charged granule molecules that can bind multiple cationic proteins

To uncover mechanisms that regulate the function of NCPs, we first conducted a systematic comparison of the physicochemical properties of the most abundant granule proteins secreted by neutrophils.[28] These proteins included 11 proteins from the primary granules, 12 from the secondary granules, 16 from the tertiary granules, and 2 from the secretory vesicles (Figure 1A). We observed that 14 of these proteins displayed a positive net charge (above +2.5 at pH 7.0) and included most of the known NCPs, 16 were rather neutral (between −2 and +2), while 11 displayed a significant negative charge (below −2.5 at pH 7.0) (Figure 1B). We then asked whether the negatively charged proteins would interact with positively charged NCPs to potentially regulate their function. We used the artificial intelligence-based 3D structure prediction tool AlphaFold to model the interaction of the 11 anionic proteins (leucyl-cystinyl aminopeptidase [LNPEP], pentraxin-related protein [PTX3], transcobalamin-1 [TCN1], matrix metalloproteinase-9 [MMP9], prostatic acid phosphatase [ACPP], plasma alpha-L-fucosidase [FUCA2], alpha-1-acid glycoprotein 2 [ORM2], OLFM4, cathepsin B [CTSB], dipeptidyl peptidase 2 [DPP2], and haptoglobin [HP]) with LL-37, a functionally well-characterized NCP. All anionic molecules except OLFM4 interacted with LL-37 and promoted its oligomerization into multimeric channels (Figure 1C), a structure required for membrane insertion and bactericidal activity.[29] By contrast, OLFM4 interaction with LL-37 did not yield such channels but resulted in the binding sequestration of each individual LL-37 monomer (Figure 1C). Binding of anionic proteins (LNPEP, PTX3, TCN1, and OLFM4) to NCPs (neutrophil gelatinase-associated lipocalin [NGAL], LL-37, and lactotransferrin [LTF]) was confirmed by ELISA (Figure 1D) and shown to require electrostatic interactions, as increasing anionic strength using heparin abolished the binding capacity (Figure S1).

OLFM4 inhibits the antimicrobial activity of neutrophils

Next, we investigated whether, due to its unique interaction prediction, OLFM4 would impair the functional activities of NCPs. We conducted a bacterial killing assay using *Staphylococcus epidermidis*, a prevalent commensal bacterium found on human skin and a target of neutrophil killing activity in injured skin.[12] LL-37 exhibited potent antimicrobial activity against *S. epidermidis*, which was specifically inhibited by addition of OLFM4 but not by other neutrophil anionic molecules (Figure 2A). OLFM4 prevented the association of LL-37 with the bacterial surface, which is a crucial step for initiating the killing process (Figure 2B). OLFM4 also abrogated the antimicrobial activity of other NCPs such as NGAL and LTF, indicating a broad inhibitory activity against NCPs (Figure 2C). As control, OLFM4 did not affect the bactericidal activity of other antimicrobial granule proteins, including myeloperoxidase (MPO) and LYZ, despite effective binding (Figures S2 and 1D), consistent with their enzymatic antibacterial mechanism. Collectively, these findings indicate that OLFM4 interacts with NCPs, and thereby controls their ability to bind microbial membranes and kill bacteria. Importantly, addition of exogenous OLFM4 to neutrophil cultures strongly inhibited killing of *S. epidermidis* without affecting neutrophil viability (Figures 2D, S3A, and S3B). The killing activity was most likely mediated by secreted NCPs, as supernatants of activated neutrophils effectively killed *S. epidermidis,* and this antimicrobial activity was again abrogated by addition of recombinant human OLFM4 (Figure 2E).

We also tested the outcome of OFM4 inhibition using neutrophils of OLFM4-deficient mice (*Olfm4*$^{-/-}$). Bone marrow-derived *Olfm4*$^{-/-}$ neutrophils exhibited greater efficiency in killing *S. epidermidis* compared to wild-type (WT) neutrophils (Figure 2F). The addition of recombinant mouse OLFM4 to *Olfm4*$^{-/-}$ neutrophils reversed the heightened antimicrobial activity, mirroring the observation with human neutrophils (Figure 2F). The increased killing activity of *Olfm4*$^{-/-}$ neutrophils persisted when neutrophil supernatants were utilized, highlighting the role of secreted NCPs (Figure 2G). In summary, these findings demonstrate that OLFM4 controls the antimicrobial response of neutrophils by binding of secreted NCPs. The antimicrobial activity can be inhibited by OLFM4 supplementation and promoted by blocking OLFM4.

OLFM4 inhibits the formation of DNA complexes and TLR9 activation of pDCs and neutrophils

Because NCPs can bind DNA and promote cellular internalization and TLR9 activation of pDCs and neutrophils,[3,12,13,16] we sought to investigate whether the binding of OLFM4 to NCPs could also inhibit this pro-inflammatory mechanism. First, we assessed the capacity of cationic neutrophil proteins to bind DNA. Consistent with previous observations, we found that, among the 4 strongly cationic proteins (NGAL, LL-37, LYZ, and LTF), only LL-37 and LYZ exerted strong DNA binding activity with significant decreased DNA stainability (Figure 3A). Importantly, preincubation of the NCPs with OLFM4 enhanced DNA stainability, indicating that it prevents the formation of NCP-DNA complexes (Figure 3A). To then investigate the functional consequences of this finding, we stimulated purified pDCs and neutrophils with complexes of DNA with the NCP LL-37 preincubated or not with OLFM4. Addition of the different neutrophil granule proteins to the cell cultures did not alter cell viability (Figures S3C and S3D). LL-37-DNA complexes induced strong IFN-α production by pDCs, which was significantly inhibited by pre-incubation of LL-37 with increasing concentrations of OLFM4 (Figures 3B

(C) 3D structures of the NCP LL-37 (brown) in the presence of the most negatively charged secreted neutrophil granule proteins (blue) predicted by AlphaFold. A 90° rotation of each 3D structure is also given underneath.

(D) Binding assay of 1 μM NGAL, LL-37, LYZ, LTF, and MPO on increasing concentrations of coated LNPEP, PTX3, TCN1, and OLFM4. BSA was used as a control. The half-maximal effective concentration (EC_{50}) of each protein is given. Data are the mean ± SEM of 3 replicates.

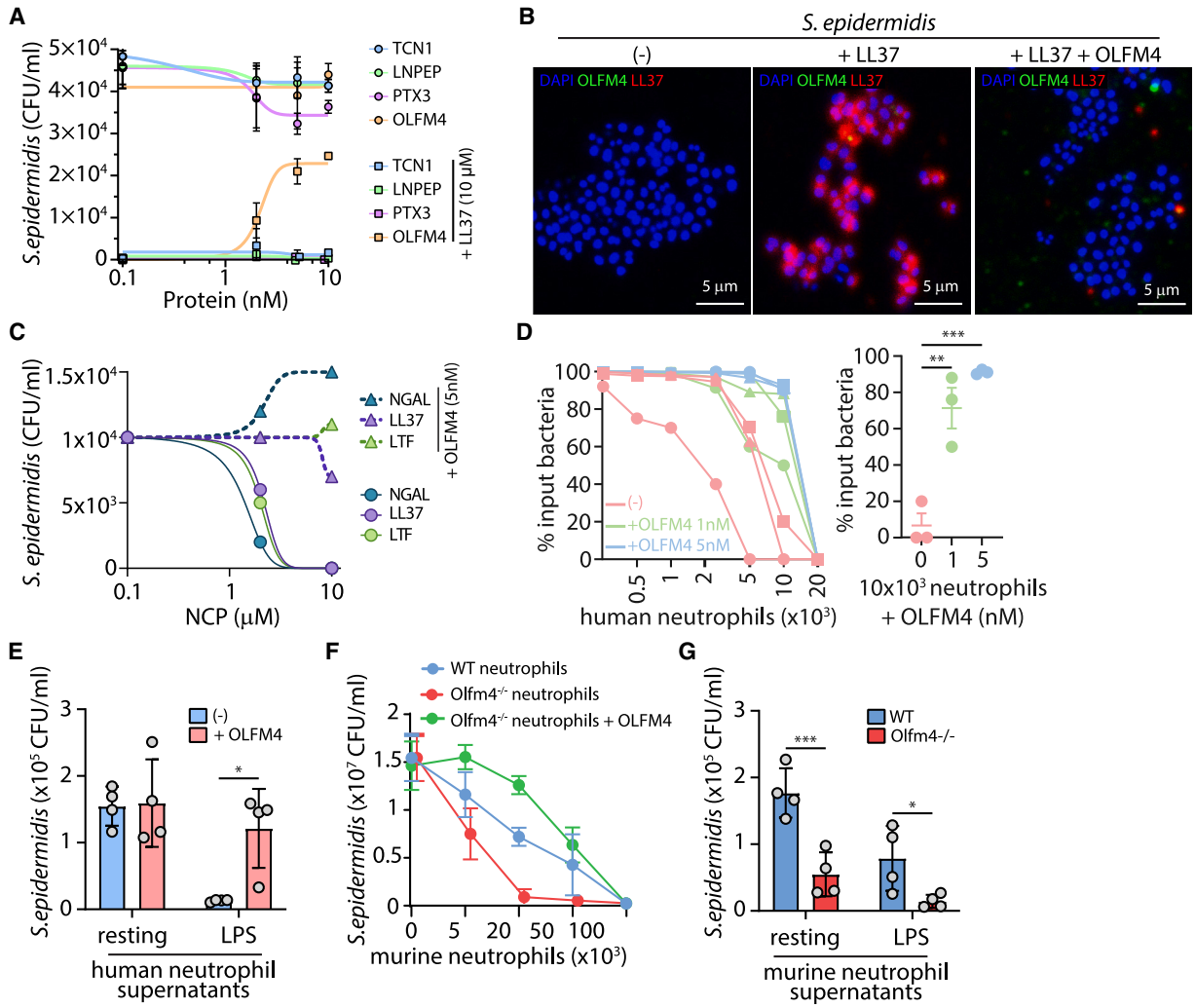

Figure 2. OLFM4 inhibits the antimicrobial activity of NCPs

(A) Growth of *S. epidermidis* in culture with increasing concentrations of the neutrophil anionic proteins TCN1, LNPEP, PTX3, and OLFM4 pre-incubated or not with 10 µM LL-37. Data are the mean ± SD of triplicates.

(B) Confocal microscopy images of *S. epidermidis* cultured for 1 h with LL-37 pre-incubated or not with OLFM4 and stained with DAPI (blue), anti-OLFM4 (green), and anti-LL-37 (red) antibodies. Scale bars represent 5 µm. Images shown are representative of three independent experiments.

(C) Growth of *S. epidermidis* in culture with increasing concentrations of the neutrophil cationic proteins (NCPs) NGAL, LL-37, and LTF pre-incubated or not with 5 nM OLFM4.

(D) Percentages of viable bacteria (*S. epidermidis*) cultured with increasing amounts of blood-isolated human neutrophils ($n = 3$) in the presence of 1 and 5 nM OLFM4 (left) and quantification of viable bacteria in the condition of 10×10^3 neutrophils (right). The p values were obtained with one-way ANOVA followed by Tukey's test. $^{**}p < 0.01$, $^{***}p < 0.001$.

(E) Quantification of viable *S. epidermidis* cultured with supernatants harvested from resting or lipopolysaccharide (LPS)-stimulated human neutrophils ($n = 4$) in the presence or absence of OLFM4. The p values were obtained with two-way ANOVA followed by Sidak's multiple comparisons test. $^{*}p < 0.05$.

(D and E) Each dot represents an individual donor.

(F) Quantification of viable *S. epidermidis* cultured with increasing amounts of murine neutrophils isolated from WT or *Olfm4*$^{-/-}$ mice in the presence or absence of OLFM4. Data are the mean ± SEM of 3 mice.

(G) Quantification of viable *S. epidermidis* cultured with supernatants harvested from resting or LPS-stimulated murine neutrophils isolated from WT ($n = 4$) or *Olfm4*$^{-/-}$ ($n = 4$) mice. The p values were obtained with two-way ANOVA followed by Sidak's multiple comparisons test. $^{*}p < 0.05$, $^{***}p < 0.001$. Each dot represents an individual mouse.

and S3E). LL-37-DNA complexes also induced tumor necrosis factor (TNF), IL-6, and CXCL8 production by human neutrophils, which was similarly inhibited by pre-incubation of LL-37 with increasing concentrations of OLFM4 (Figures 3C and S3F). Accordingly, LL-37-DNA complexes induced significantly higher levels of TNF, IL-6, and IFNγ in OLFM4-deficient neutrophils from *Olfm4*$^{-/-}$ mice when compared to neutrophils isolated from WT mice (Figure 3D). Altogether, these data suggest that

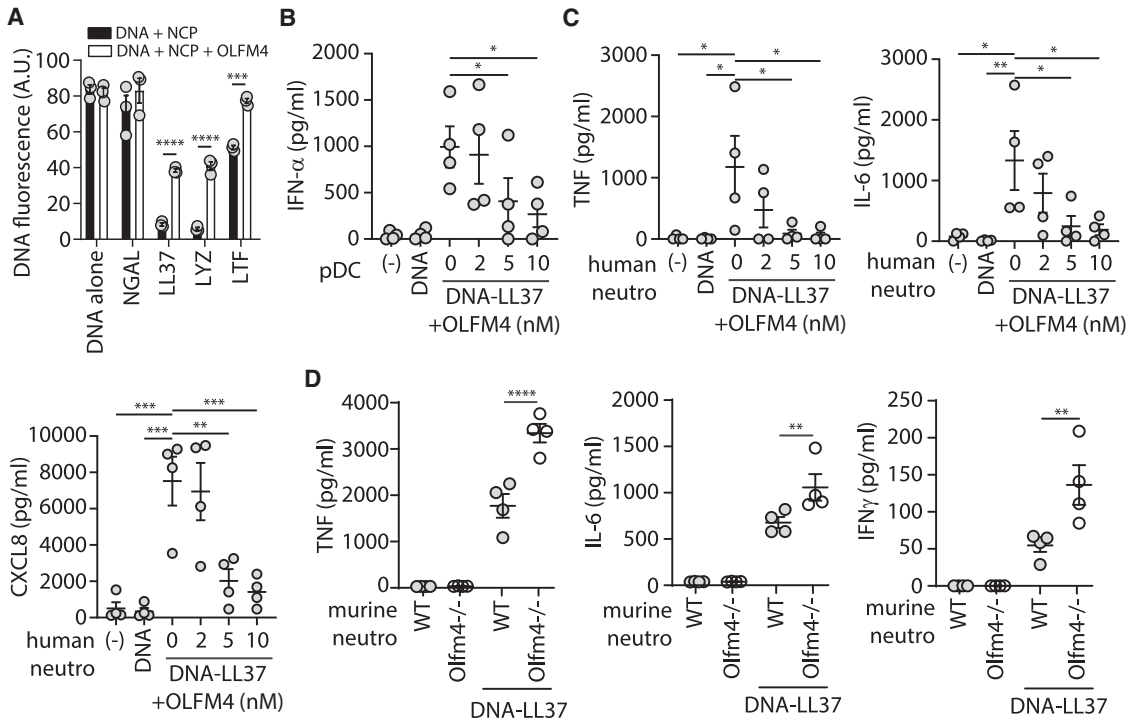

Figure 3. OLFM4 inhibits the formation of DNA complexes and TLR9 activation of pDCs and neutrophils

(A) Fluorimetric quantification of DNA staining by picogreen dye after mixing of bacterial DNA with NGAL, LL-37, LYZ, or LTF pre-incubated or not with OLFM4. The *p* values were obtained with two-way ANOVA followed by Sidak's multiple comparisons test. $^{**}p < 0.01$, $^{***}p < 0.001$, $^{****}p < 0.0001$. Experiments were performed at least 3 times.

(B) IFN-α produced by human pDCs stimulated overnight with LL-37-bacterial DNA complexes in the presence of increasing concentrations of OLFM4.

(C) TNF, IL-6, and CXCL8 produced by human neutrophils stimulated overnight with LL-37-bacterial DNA complexes in the presence of increasing concentrations of OLFM4.

(B and C) Each dot represents an individual donor. The *p* values were obtained with one-way ANOVA followed by Tukey's test. $^{*}p < 0.05$, $^{**}p < 0.01$, $^{***}p < 0.001$.

(D) TNF, IL-6, and IFN-γ produced by murine neutrophils isolated from WT ($n = 4$) or *Olfm4*$^{-/-}$ ($n = 4$) mice stimulated overnight or not with LL-37-bacterial DNA complexes. The *p* values were obtained with two-way ANOVA followed by Sidak's multiple comparisons test. $^{**}p < 0.01$, $^{****}p < 0.0001$.

OLFM4 inhibited the ability of cationic neutrophil proteins to form complexes with self- and bacterial DNA and to promote DNA immunogenicity.

OLFM4 regulates antimicrobial and inflammatory responses in skin wounds

After establishing that OLFM4 inhibits both the antimicrobial activity and DNA immunogenicity of NCPs, we aimed to evaluate the relevance of this discovery *in vivo* using a murine model of skin injury. This model relies on both the antimicrobial and DNA complex formation abilities of NCPs for epidermal repair.[12,11] In this model, injury of *Olfm4*$^{-/-}$ mice led to a rapid reduction in the total number of skin commensals within the wound compared to injured WT mice (Figure 4A). Microbial profiling unveiled a significant and sustained depletion of *Staphylococcus* species, the predominant commensal species in skin wounds, in *Olfm4*$^{-/-}$ mice compared to WT mice (Figure 4B), indicating enhanced *in vivo* antimicrobial activity in the absence of OLFM4. Furthermore, transcriptomic analysis of the wounds revealed robust expression of type I IFN and IFN-stimulated genes in *Olfm4*$^{-/-}$ mice compared to WT mice (Figure 4C), suggesting increased formation of DNA complexes with potent activation of pDCs in wounds lacking OLFM4. We also observed elevated gene expression levels of the pro-inflammatory cytokines *Tnf*, *Il6*, and *Ifng* in OLFM4-deficient wounds (Figure 4C), likely associated with the enhanced sensing of DNA complexes by neutrophils (Figure 3D). Last, we noted a marked acceleration of wound re-epithelialization in *Olfm4*$^{-/-}$ mice, starting as early as 2 days post injury. Overall, the wound closure process lasted 6 days in the *Olfm4*$^{-/-}$ mice compared to 8 days in WT mice (Figures 4D–4F). These findings highlight the *in vivo* regulatory roles of OLFM4 in antimicrobial and inflammatory responses and suggest that blocking OLFM4 could serve as a strategy to accelerate wound healing in the skin.

DISCUSSION

By investigating the physicochemical properties of neutrophil granule proteins, we found that the secreted negatively charged protein OLFM4 possesses a unique structure enabling its binding to positively charged NCPs and preventing NCP oligomerization. This interaction has a profound impact, as it prevents NCPs from carrying out their essential functions of killing bacteria and forming immunogenic complexes with

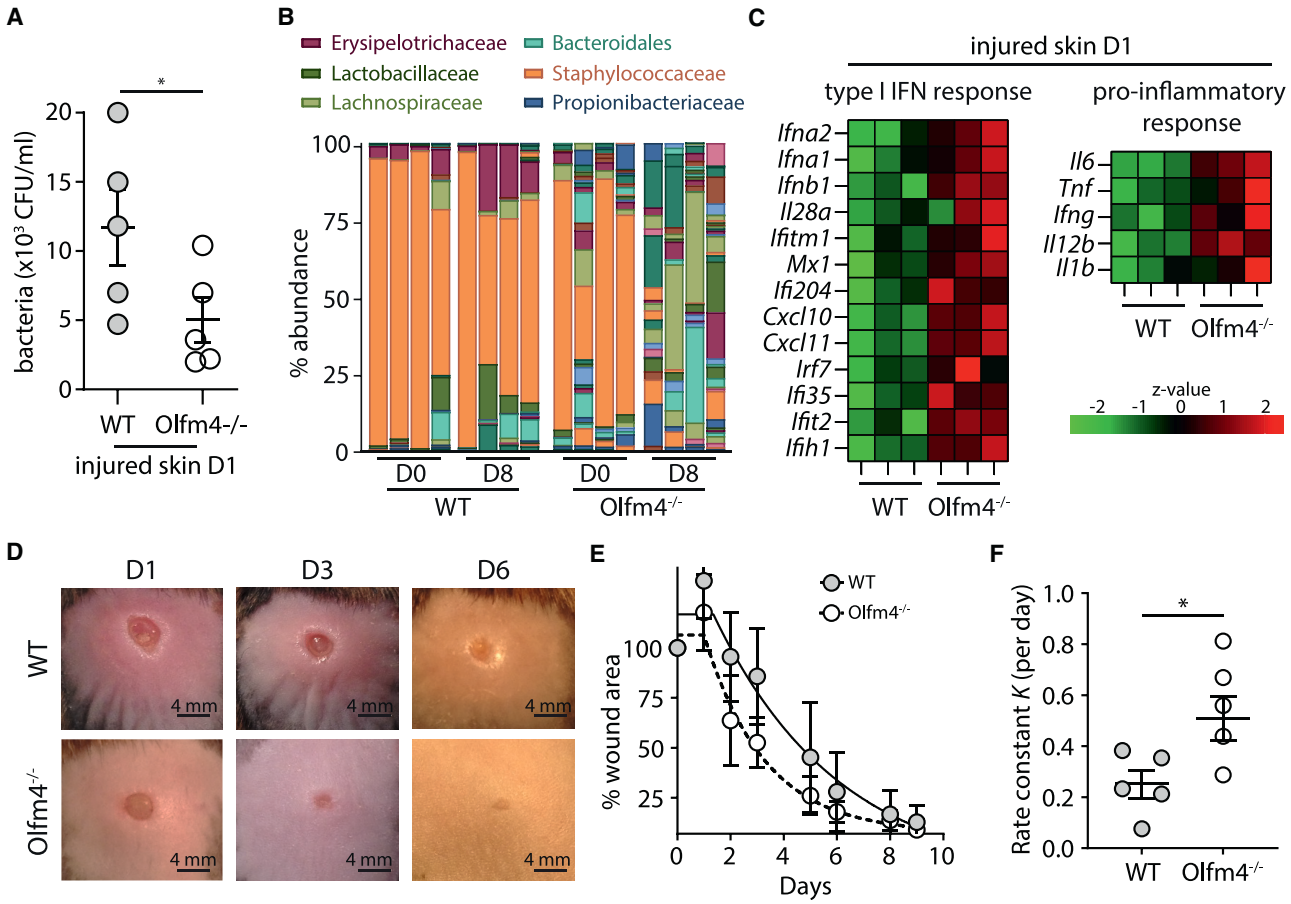

Figure 4. OLFM4 inhibits antimicrobial and inflammatory responses *in vivo*

(A) Number of bacterial colony forming units (CFUs) after overnight culture of skin lesions harvested from WT and *Olfm4*$^{-/-}$ mice 1 day after injury. The *p* values were obtained with Student's t test. *$p < 0.05$.

(B) Bacterial profiling of uninjured (day 0) and injured (day 8) skin in WT ($n = 4$) and *Olfm4*$^{-/-}$ ($n = 4$) mice measured by 16S rDNA sequencing. Relative abundances of the main bacterial families are shown. Data shown are representative of two independent experiments.

(C) Expression profiles of type I IFN response and pro-inflammatory genes in skin of WT ($n = 3$) and *Olfm4*$^{-/-}$ ($n = 3$) mice harvested 24 h following injury, assessed by Nanostring. Data are presented as a heatmap of z values.

(D) Photographs of skin wounds in WT and *Olfm4*$^{-/-}$ mice 1 day, 3 days, and 6 days post injury. Scale bars represent 4 mm.

(E) Wound closure kinetics shown as percentage of initial wound size in the different mouse groups ($n = 5$) as in (D). Data are the mean ± SD of five mice per group and are representative of 2 independent experiments.

(F) Rate at which the wounds are closing in WT and *Olfm4*−/− mice, expressed as the constant K ($n = 5$). The *p* values were obtained with one-way ANOVA followed by Tukey's test. *$p < 0.05$.

DNA. Consequently, the pro-inflammatory functions of neutrophils are inhibited due to the lack of NCP-mediated activation of intracellular DNA receptors in immune cells such as pDCs and neutrophils.

In our previous work, we have described the pivotal role of NCP activity in the initiation of physiological skin repair mechanisms through activation of TLR9 in pDCs.[12] Here, we now demonstrate that inhibition of OLFM4 can induce a remarkable elevation of this NCP activity, surpassing physiological levels. This phenomenon results in accelerated wound healing in normal skin, offering promising therapeutic avenues for enhancing tissue regeneration in healthy individuals. Nevertheless, it is imperative to acknowledge the delicate equilibrium between promoting enhanced repair responses and triggering chronic inflammation. Excessive NCP activity is implicated in various chronic inflammatory skin conditions, such as plaque psoriasis,[16] pustular psoriasis,[13] cutaneous lupus,[10,30], rosacea,[31] and dermatomyositis.[32] In such instances, therapeutic intervention with exogenous OLFM4 may effectively attenuate the exaggerated neutrophil-mediated inflammatory response and prevent the progression of the disease. These insights underscore the great potential of targeting OLFM4 for therapeutic modulation of NCP activity but also emphasize the delicate interplay between tissue repair mechanisms and inflammatory processes.

OLFM4 inhibits the antimicrobial activity of various NCPs, each employing distinct antimicrobial mechanisms. For instance, LL-37 disrupts bacterial membranes due to its cationic amphipathic nature,[33] while NGAL primarily controls

bacterial growth by capturing and sequestering essential iron necessary for bacterial proliferation without requiring a positive net charge.[34] LTF, on the other hand, possesses both activities.[7] Thus, it appears that OLFM4 not only impedes the antimicrobial function of NCPs by neutralizing their cationic residues but may also physically restrains these molecules, preventing them from interacting with their molecular targets.

The evolutionary purpose of OLFM4 as a direct inhibitor of the antibacterial activity may be a balance between allowing the survival of commensal bacteria while maintaining effective protection against infection. Indeed, we observed that the absence of OLFM4 favors the killing of skin commensal bacterial species (e.g., *Staphylococcus* species), which may ultimately lead to microbial dysbiosis and increase the risk of pathogen colonization in the long term. One way to control this balance is to control the ratio between OLFM4 and the antimicrobial NCPs. This may be achieved by the singular expression of OLFM4 in a subset of neutrophils. Only 10% to 30% of blood neutrophils in humans and 7% to 35% in mice can produce OLFM4.[21,35] This expression regulation at the single-cell level may help control the production of OLFM4 in terms of timing and location by differential activation of these two subsets; however, no differences in the recruitment or activation of these two neutrophil subsets have been identified so far.[36]

OLFM4 also inhibits proinflammatory functions of NCPs, in part through inhibition of DNA binding and activation of intracellular DNA sensors such as TLR9. However, other pro-inflammatory functions of NCP have been described, including receptor-dependent activities. LL-37 has been shown to attract immune cells to the site of infection, enhance the phagocytic activity of immune cells, and induce IL-1β production by activating various receptors, including N-formyl peptide receptors (FPR1/2),[37] the Mac-1 receptor,[38] and the purinergic P2X7 receptor.[39] On the other hand, NGAL and LTF can be internalized by host cells via receptors that facilitate the absorption of iron ions,[40,41] contributing to iron homeostasis. It is likely that similar physical restraint by OLFM4 prevents the interaction of NCPs with these molecular targets.

A recent study has identified that certain proteins of severe acute respiratory syndrome coronavirus 2 (SARS-CoV-2) share cationic properties and structural features with NCPs such as LL-37. These proteins can assemble the viral genome into immunogenic complexes,[42] contributing to detrimental inflammatory responses observed in COVID-19. OLFM4 may have the capacity to disrupt these complexes, providing a potential strategy to treat inflammatory responses associated with COVID-19.

At the basal level, OLFM4 is typically not present in most tissues, including the skin. However, it is constitutively expressed by epithelial stem cells in the small intestine, the colon, and the prostate.[20] In these organs, epithelial OLFM4 inhibits cell proliferation through the regulation of Wnt/β-catenin and hedgehog signaling pathways.[43,44] While gut epithelial OLFM4 regulates cell proliferation under normal conditions, maintaining tissue homeostasis, OLFM4 derived from neutrophils appears to primarily modulate bacterial elimination and inflammatory responses upon barrier breach.[45] In line with this, the absence of OLFM4 expression in gut epithelial cells has been linked to intestinal carcinogenesis, possibly mediated by heightened activation of Wnt and NF-κB pathways.[44,46] Conversely, OLFM4 expression has been found to be increased in the inflamed colon of patients with Crohn's disease and ulcerative colitis,[47] suggesting a potential link with a diminished ability to eliminate bacteria and an elevated risk of pathobiont proliferation.

In conclusion, our research highlights the regulatory role of OLFM4 on the antimicrobial and inflammatory functions of NCPs. The addition of exogenous OLFM4 inhibits NCP activity, whereas its neutralization enhances NCP activity, promoting tissue reepithelialization beyond physiological levels. These findings suggest OLFM4 as a potential therapeutic target for inflammatory diseases or for accelerating wound repair.

Limitations of the study

This study demonstrates that OLFM4 binds to NCPs, inhibiting their oligomerization and subsequent antibacterial and pro-inflammatory functions. However, the findings are constrained by the experimental approach. The *in silico* predictions of 3D structure and *in vitro* binding assays focus on the interaction between a single negatively charged molecule and one NCP, whereas, in reality, neutrophils release hundreds of granule proteins simultaneously, leading to more complex protein-protein interactions that would require different modeling approaches. Additionally, the analyses did not account for extracellular matrix components present in tissues that could influence protein binding capacities *in vivo*. The study also only tested the inhibitory activity of OLFM4 on pro-inflammatory cytokine production by immune cells following NCP-DNA stimulation; the potential impact on other immune and non-immune cell functions remains to be determined. Last, while the regulatory role of exogenous OLFM4 was assessed *in vitro*, it has not been examined *in vivo* and requires further investigation to confirm its potential use for therapy.

RESOURCE AVAILABILITY

Lead contact

Requests for further information and resources should be directed to and will be fulfilled by the lead contact, Jeremy Di Domizio (Jeremy.di-domizio@chuv.ch).

Material availability

This study did not generate new unique reagents.

Data and code availability

- All data reported in this paper will be shared by the lead contact upon request.
- This paper does not report original code.
- Any additional information required to reanalyze the data reported in this paper is available from the lead contact upon request.

ACKNOWLEDGMENTS

We thank A. Joncic and I. Surbeck for technical assistance. This work was funded by an MD-PhD training grant from the University of Lausanne (to S.V.-D.), the Swiss National Science Foundation (310030B_182834 and 310030_204835 to M.G.), and a grant from Novartis Stiftung für Medizinisch-Biologische Forschung (to J.D.D.).

AUTHOR CONTRIBUTIONS

S.V.-D. and J.D.D. performed the experiments. M.G. and J.D.D. conceived, designed, and evaluated the study and jointly wrote the manuscript.

DECLARATION OF INTERESTS

The authors declare no competing interests.

STAR★METHODS

Detailed methods are provided in the online version of this paper and include the following:

- KEY RESOURCES TABLE
- EXPERIMENTAL MODEL AND STUDY PARTICIPANT DETAILS
  - Human healthy blood samples
  - Murine skin injury model
- METHOD DETAILS
  - Protein net charge determination
  - Prediction of protein structures and interaction
  - ELISA binding assay
  - Antimicrobial assays
  - Imaging of NCP binding to bacteria
  - DNA condensation assay
  - Isolation and stimulation of neutrophils and pDCs
  - Gene expression profiling
- QUANTIFICATION AND STATISTICAL ANALYSIS

SUPPLEMENTAL INFORMATION

Supplemental information can be found online at https://doi.org/10.1016/j.celrep.2024.114863.

Received: May 8, 2024
Revised: August 30, 2024
Accepted: September 25, 2024
Published: October 11, 2024

REFERENCES

1. Zasloff, M. (2002). Antimicrobial peptides of multicellular organisms. Nature *415*, 389–395. https://doi.org/10.1038/415389a.
2. Lai, Y., and Gallo, R.L. (2009). AMPed up immunity: how antimicrobial peptides have multiple roles in immune defense. Trends Immunol. *30*, 131–141. https://doi.org/10.1016/j.it.2008.12.003.
3. Lande, R., Gregorio, J., Facchinetti, V., Chatterjee, B., Wang, Y.H., Homey, B., Cao, W., Wang, Y.H., Su, B., Nestle, F.O., et al. (2007). Plasmacytoid dendritic cells sense self-DNA coupled with antimicrobial peptide. Nature *449*, 564–569. https://doi.org/10.1038/nature06116.
4. Larrick, J.W., Hirata, M., Balint, R.F., Lee, J., Zhong, J., and Wright, S.C. (1995). Human CAP18: a novel antimicrobial lipopolysaccharide-binding protein. Infect. Immun. *63*, 1291–1297. https://doi.org/10.1128/iai.63.4.1291-1297.1995.
5. Ganz, T. (2003). Defensins: antimicrobial peptides of innate immunity. Nat. Rev. Immunol. *3*, 710–720. https://doi.org/10.1038/nri1180.
6. Zhang, H., Fu, G., and Zhang, D. (2014). Cloning, characterization, and production of a novel lysozyme by different expression hosts. J. Microbiol. Biotechnol. *24*, 1405–1412. https://doi.org/10.4014/jmb.1404.04039.
7. Gruden, Š., and Poklar Ulrih, N. (2021). Diverse Mechanisms of Antimicrobial Activities of Lactoferrins, Lactoferricins, and Other Lactoferrin-Derived Peptides. Int. J. Mol. Sci. *22*, 11264. https://doi.org/10.3390/ijms222011264.
8. Chamilos, G., Gregorio, J., Meller, S., Lande, R., Kontoyiannis, D.P., Modlin, R.L., and Gilliet, M. (2012). Cytosolic sensing of extracellular self-DNA transported into monocytes by the antimicrobial peptide LL37. Blood *120*, 3699–3707. https://doi.org/10.1182/blood-2012-01-401364.
9. Meller, S., Di Domizio, J., Voo, K.S., Friedrich, H.C., Chamilos, G., Ganguly, D., Conrad, C., Gregorio, J., Le Roy, D., Roger, T., et al. (2015). T(H)17 cells promote microbial killing and innate immune sensing of DNA via interleukin 26. Nat. Immunol. *16*, 970–979. https://doi.org/10.1038/ni.3211.
10. Lande, R., Ganguly, D., Facchinetti, V., Frasca, L., Conrad, C., Gregorio, J., Meller, S., Chamilos, G., Sebasigari, R., Riccieri, V., et al. (2011). Neutrophils activate plasmacytoid dendritic cells by releasing self-DNA-peptide complexes in systemic lupus erythematosus. Sci. Transl. Med. *3*, 73ra19. https://doi.org/10.1126/scitranslmed.3001180.
11. Gregorio, J., Meller, S., Conrad, C., Di Nardo, A., Homey, B., Lauerma, A., Arai, N., Gallo, R.L., Digiovanni, J., and Gilliet, M. (2010). Plasmacytoid dendritic cells sense skin injury and promote wound healing through type I interferons. J. Exp. Med. *207*, 2921–2930. https://doi.org/10.1084/jem.20101102.
12. Di Domizio, J., Belkhodja, C., Chenuet, P., Fries, A., Murray, T., Mondéjar, P.M., Demaria, O., Conrad, C., Homey, B., Werner, S., et al. (2020). The commensal skin microbiota triggers type I IFN-dependent innate repair responses in injured skin. Nat. Immunol. *21*, 1034–1045. https://doi.org/10.1038/s41590-020-0721-6.
13. Baldo, A., Di Domizio, J., Yatim, A., Vandenberghe-Dürr, S., Jenelten, R., Fries, A., Grizzetti, L., Kuonen, F., Paul, C., Modlin, R.L., et al. (2024). Human neutrophils drive skin autoinflammation by releasing interleukin (IL)-26. J. Exp. Med. *221*, e20231464. https://doi.org/10.1084/jem.20231464.
14. Büchau, A.S., and Gallo, R.L. (2007). Innate immunity and antimicrobial defense systems in psoriasis. Clin. Dermatol. *25*, 616–624. https://doi.org/10.1016/j.clindermatol.2007.08.016.
15. Hollox, E.J., Huffmeier, U., Zeeuwen, P.L.J.M., Palla, R., Lascorz, J., Rodijk-Olthuis, D., van de Kerkhof, P.C.M., Traupe, H., de Jongh, G., den Heijer, M., et al. (2008). Psoriasis is associated with increased beta-defensin genomic copy number. Nat. Genet. *40*, 23–25. https://doi.org/10.1038/ng.2007.48.
16. Lande, R., Chamilos, G., Ganguly, D., Demaria, O., Frasca, L., Durr, S., Conrad, C., Schröder, J., and Gilliet, M. (2015). Cationic antimicrobial peptides in psoriatic skin cooperate to break innate tolerance to self-DNA. Eur. J. Immunol. *45*, 203–213. https://doi.org/10.1002/eji.201344277.
17. Vordenbäumen, S., Fischer-Betz, R., Timm, D., Sander, O., Chehab, G., Richter, J., Bleck, E., and Schneider, M. (2010). Elevated levels of human beta-defensin 2 and human neutrophil peptides in systemic lupus erythematosus. Lupus *19*, 1648–1653. https://doi.org/10.1177/0961203310377089.
18. Diana, J., Simoni, Y., Furio, L., Beaudoin, L., Agerberth, B., Barrat, F., and Lehuen, A. (2013). Crosstalk between neutrophils, B-1a cells and plasmacytoid dendritic cells initiates autoimmune diabetes. Nat. Med. *19*, 65–73. https://doi.org/10.1038/nm.3042.
19. Zhang, Z., Meng, P., Han, Y., Shen, C., Li, B., Hakim, M.A., Zhang, X., Lu, Q., Rong, M., and Lai, R. (2015). Mitochondrial DNA-LL-37 Complex Promotes Atherosclerosis by Escaping from Autophagic Recognition. Immunity *43*, 1137–1147. https://doi.org/10.1016/j.immuni.2015.10.018.
20. Zhang, J., Liu, W.L., Tang, D.C., Chen, L., Wang, M., Pack, S.D., Zhuang, Z., and Rodgers, G.P. (2002). Identification and characterization of a novel member of olfactomedin-related protein family, hGC-1, expressed during myeloid lineage development. Gene *283*, 83–93. https://doi.org/10.1016/s0378-1119(01)00763-6.
21. Clemmensen, S.N., Bohr, C.T., Rørvig, S., Glenthøj, A., Mora-Jensen, H., Cramer, E.P., Jacobsen, L.C., Larsen, M.T., Cowland, J.B., Tanassi, J.T., et al. (2012). Olfactomedin 4 defines a subset of human neutrophils. J. Leukoc. Biol. *91*, 495–500. https://doi.org/10.1189/jlb.0811417.
22. Lee, H.J., Georgiadou, A., Walther, M., Nwakanma, D., Stewart, L.B., Levin, M., Otto, T.D., Conway, D.J., Coin, L.J., and Cunnington, A.J. (2018). Integrated pathogen load and dual transcriptome analysis of

systemic host-pathogen interactions in severe malaria. Sci. Transl. Med. *10*, eaar3619. https://doi.org/10.1126/scitranslmed.aar3619.

23. Kangelaris, K.N., Clemens, R., Fang, X., Jauregui, A., Liu, T., Vessel, K., Deiss, T., Sinha, P., Leligdowicz, A., Liu, K.D., et al. (2021). A neutrophil subset defined by intracellular olfactomedin 4 is associated with mortality in sepsis. Am. J. Physiol. Lung Cell Mol. Physiol. *320*, L892–L902. https://doi.org/10.1152/ajplung.00090.2020.
24. Alder, M.N., Opoka, A.M., Lahni, P., Hildeman, D.A., and Wong, H.R. (2017). Olfactomedin-4 Is a Candidate Marker for a Pathogenic Neutrophil Subset in Septic Shock. Crit. Care Med. *45*, e426–e432. https://doi.org/10.1097/CCM.0000000000002102.
25. Liu, W., Yan, M., Liu, Y., McLeish, K.R., Coleman, W.G., Jr., and Rodgers, G.P. (2012). Olfactomedin 4 inhibits cathepsin C-mediated protease activities, thereby modulating neutrophil killing of Staphylococcus aureus and Escherichia coli in mice. J. Immunol. *189*, 2460–2467. https://doi.org/10.4049/jimmunol.1103179.
26. Liu, W., Yan, M., Sugui, J.A., Li, H., Xu, C., Joo, J., Kwon-Chung, K.J., Coleman, W.G., and Rodgers, G.P. (2013). Olfm4 deletion enhances defense against Staphylococcus aureus in chronic granulomatous disease. J. Clin. Invest. *123*, 3751–3755. https://doi.org/10.1172/JCI68453.
27. Liu, W., Yan, M., Liu, Y., Wang, R., Li, C., Deng, C., Singh, A., Coleman, W.G., Jr., and Rodgers, G.P. (2010). Olfactomedin 4 down-regulates innate immunity against Helicobacter pylori infection. Proc. Natl. Acad. Sci. USA *107*, 11056–11061. https://doi.org/10.1073/pnas.1001269107.
28. Rørvig, S., Ostergaard, O., Heegaard, N.H., and Borregaard, N. (2013). Proteome profiling of human neutrophil granule subsets, secretory vesicles, and cell membrane: correlation with transcriptome profiling of neutrophil precursors. J. Leukoc. Biol. *94*, 711–721. https://doi.org/10.1189/jlb.1212619.
29. Sancho-Vaello, E., Gil-Carton, D., François, P., Bonetti, E.J., Kreir, M., Pothula, K.R., Kleinekathöfer, U., and Zeth, K. (2020). The structure of the antimicrobial human cathelicidin LL-37 shows oligomerization and channel formation in the presence of membrane mimics. Sci. Rep. *10*, 17356. https://doi.org/10.1038/s41598-020-74401-5.
30. Gestermann, N., Di Domizio, J., Lande, R., Demaria, O., Frasca, L., Feldmeyer, L., Di Lucca, J., and Gilliet, M. (2018). Netting Neutrophils Activate Autoreactive B Cells in Lupus. J. Immunol. *200*, 3364–3371. https://doi.org/10.4049/jimmunol.1700778.
31. Mylonas, A., Hawerkamp, H.C., Wang, Y., Chen, J., Messina, F., Demaria, O., Meller, S., Homey, B., Di Domizio, J., Mazzolai, L., et al. (2023). Type I IFNs link skin-associated dysbiotic commensal bacteria to pathogenic inflammation and angiogenesis in rosacea. JCI Insight *8*, e151846. https://doi.org/10.1172/jci.insight.151846.
32. Lu, X., Tang, Q., Lindh, M., Dastmalchi, M., Alexanderson, H., Popovic Silwerfeldt, K., Agerberth, B., Lundberg, I.E., and Wick, C. (2017). The host defense peptide LL-37 a possible inducer of the type I interferon system in patients with polymyositis and dermatomyositis. J. Autoimmun. *78*, 46–56. https://doi.org/10.1016/j.jaut.2016.12.003.
33. Henzler Wildman, K.A., Lee, D.K., and Ramamoorthy, A. (2003). Mechanism of lipid bilayer disruption by the human antimicrobial peptide, LL-37. Biochemistry *42*, 6545–6558. https://doi.org/10.1021/bi0273563.
34. Goetz, D.H., Holmes, M.A., Borregaard, N., Bluhm, M.E., Raymond, K.N., and Strong, R.K. (2002). The neutrophil lipocalin NGAL is a bacteriostatic agent that interferes with siderophore-mediated iron acquisition. Mol. Cell *10*, 1033–1043. https://doi.org/10.1016/s1097-2765(02)00708-6.
35. Alder, M.N., Mallela, J., Opoka, A.M., Lahni, P., Hildeman, D.A., and Wong, H.R. (2019). Olfactomedin 4 marks a subset of neutrophils in mice. Innate Immun. *25*, 22–33. https://doi.org/10.1177/1753425918817611.
36. Welin, A., Amirbeagi, F., Christenson, K., Björkman, L., Björnsdottir, H., Forsman, H., Dahlgren, C., Karlsson, A., and Bylund, J. (2013). The human neutrophil subsets defined by the presence or absence of OLFM4 both transmigrate into tissue in vivo and give rise to distinct NETs in vitro. PLoS One *8*, e69575. https://doi.org/10.1371/journal.pone.0069575.
37. De, Y., Chen, Q., Schmidt, A.P., Anderson, G.M., Wang, J.M., Wooters, J., Oppenheim, J.J., and Chertov, O. (2000). LL-37, the neutrophil granule- and epithelial cell-derived cathelicidin, utilizes formyl peptide receptor-like 1 (FPRL1) as a receptor to chemoattract human peripheral blood neutrophils, monocytes, and T cells. J. Exp. Med. *192*, 1069–1074. https://doi.org/10.1084/jem.192.7.1069.
38. Lishko, V.K., Moreno, B., Podolnikova, N.P., and Ugarova, T.P. (2016). Identification of Human Cathelicidin Peptide LL-37 as a Ligand for Macrophage Integrin alpha(M)beta(2) (Mac-1, CD11b/CD18) that Promotes Phagocytosis by Opsonizing Bacteria. Res. Rep. Biochem. *2016*, 39–55. https://doi.org/10.2147/rrbc.s107070.
39. Elssner, A., Duncan, M., Gavrilin, M., and Wewers, M.D. (2004). A novel P2X7 receptor activator, the human cathelicidin-derived peptide LL37, induces IL-1 beta processing and release. J. Immunol. *172*, 4987–4994. https://doi.org/10.4049/jimmunol.172.8.4987.
40. Yang, J., Goetz, D., Li, J.Y., Wang, W., Mori, K., Setlik, D., Du, T., Erdjument-Bromage, H., Tempst, P., Strong, R., and Barasch, J. (2002). An iron delivery pathway mediated by a lipocalin. Mol. Cell *10*, 1045–1056. https://doi.org/10.1016/s1097-2765(02)00710-4.
41. Suzuki, Y.A., Lopez, V., and Lönnerdal, B. (2005). Mammalian lactoferrin receptors: structure and function. Cell. Mol. Life Sci. *62*, 2560–2575. https://doi.org/10.1007/s00018-005-5371-1.
42. Zhang, Y., Bharathi, V., Dokoshi, T., de Anda, J., Ursery, L.T., Kulkarni, N.N., Nakamura, Y., Chen, J., Luo, E.W.C., Wang, L., et al. (2024). Viral afterlife: SARS-CoV-2 as a reservoir of immunomimetic peptides that reassemble into proinflammatory supramolecular complexes. Proc. Natl. Acad. Sci. USA *121*, e2300644120. https://doi.org/10.1073/pnas.2300644120.
43. Li, H., Liu, W., Chen, W., Zhu, J., Deng, C.X., and Rodgers, G.P. (2015). Olfactomedin 4 deficiency promotes prostate neoplastic progression and is associated with upregulation of the hedgehog-signaling pathway. Sci. Rep. *5*, 16974. https://doi.org/10.1038/srep16974.
44. Liu, W., Li, H., Hong, S.H., Piszczek, G.P., Chen, W., and Rodgers, G.P. (2016). Olfactomedin 4 deletion induces colon adenocarcinoma in Apc(-Min/+) mice. Oncogene *35*, 5237–5247. https://doi.org/10.1038/onc.2016.58.
45. Levinsky, N.C., Mallela, J., Opoka, A.M., Harmon, K., Lewis, H.V., Zingarelli, B., Wong, H.R., and Alder, M.N. (2019). The olfactomedin-4 positive neutrophil has a role in murine intestinal ischemia/reperfusion injury. Faseb. J. *33*, 13660–13668. https://doi.org/10.1096/fj.201901231R.
46. Liu, W., Liu, Y., Zhu, J., Wright, E., Ding, I., and Rodgers, G.P. (2008). Reduced hGC-1 protein expression is associated with malignant progression of colon carcinoma. Clin. Cancer Res. *14*, 1041–1049. https://doi.org/10.1158/1078-0432.CCR-07-4125.
47. Shinozaki, S., Nakamura, T., Iimura, M., Kato, Y., Iizuka, B., Kobayashi, M., and Hayashi, N. (2001). Upregulation of Reg 1alpha and GW112 in the epithelium of inflamed colonic mucosa. Gut *48*, 623–629. https://doi.org/10.1136/gut.48.5.623.

STAR★METHODS

KEY RESOURCES TABLE

REAGENT or RESOURCE	SOURCE	IDENTIFIER
Antibodies		
anti-LNPEP	Sigma Aldrich	HPA043642; RRID: AB_10964137
anti-human LL-37	Santa Cruz Biotechnology	sc-166770; RRID: AB_2068692
anti-PTX3	Sigma Aldrich	SAB4502545; RRID: AB_10745766
anti–OLFM4	Sigma Aldrich	HPA077718; RRID: AB_2732358
anti-TCN1	Sigma Aldrich	SAB1411335; RRID: AB_10795293
Bacterial and virus strains		
Staphylococcus epidermidis	ATCC	ATCC12228
Chemicals, peptides, and recombinant proteins		
LNPEP	LubioScience	ABX654174
PTX3	Abcam	ab283455
TCN1	Abcam	ab236331
Human OLFM4	LSBio	LS-G97738
Murine OLFM4	LSBio	LS-G11718
NGAL	Sigma-Aldrich	SRP6465
LL-37	Proteogenix	Custom
LTF	Sigma-Aldrich	L4894
Critical commercial assays		
nCounter murine Host Response panel	Nanostring Technologies	#115000486
EasySep™ Mouse Neutrophil Enrichment Kit	StemCell	#19762
EasySep™ Direct Human Neutrophils Isolation Kit	StemCell	#19666
EasySep™ Direct Human pDC Isolation Kit	StemCell	#17977
Experimental models: Organisms/strains		
OLFM4.KO mice	Taconic Biosciences	TF3507
Software and algorithms		
R Studio 2024.04.2–764	–	N/A
GraphPad Prism 9.0	–	N/A
nSolver 4.0	–	N/A

EXPERIMENTAL MODEL AND STUDY PARTICIPANT DETAILS

Human healthy blood samples

Studies were approved by the institutional review board of the Lausanne University Hospital and the Interregional Blood Transfusion Center, Bern, Switzerland, in accordance with the Helsinki Declaration (Project P_085). Informed consent was obtained from all healthy donors for the use of blood tubes and buffy coats.

Murine skin injury model

All animal experiments were performed according to institutional guidelines and Swiss federal and cantonal laws on animal protection (Authorization #VD2936). WT C57BL/6 mice were purchased from Charles River and Olfm4−/− (TF3507) mice were recovered from Taconic cryoarchive and rederived onto the C57BL/6 background. All animal experiments were conducted on 6–14-week-old female mice. Mice backs were shaved and depilated (Veet, Reckitt Benckiser) immediately before injury. Full-thickness injury was performed using one 4-mm punch biopsy per mouse. Closure of the wounds was then monitored daily by measuring the diameter. Wound areas were calculated as $\pi \times R2$. Data were plotted as percentages of the initial wound area (100%) and the rate of wound closure was calculated using the constant K of a one-phase decay model of curve fitting.

METHOD DETAILS

Protein net charge determination

The amino acid sequences of each secreted granule protein were retrieved by running the R function getUniProt{protr} using the UniProt IDs of proteins. Then, to compute the theoretical net charge of each protein sequence, the R function charge{Peptides} was run using the 9 different pKa scales "Bjellqvist", "Dawson", "EMBOSS", "Lehninger", "Murray", "Rodwell", "Sillero", "Solomon", and "Stryer".

Prediction of protein structures and interaction

AlphaFold was used to predict the three-dimensional structures of the interaction between different negatively charged molecules and LL-37 at a 1:4 ratio (4 anionic molecules and 16 LL-37 molecules) using the amino acid sequences of the mature proteins from NCBI's Protein resources. The AlphaFold pipeline was run using default settings, which included multiple sequence alignment (MSA) generation and model building steps. The tool leverages evolutionary information and structural templates to predict the most likely conformation of the protein. Molecular visualization of the predicted structures was generated by running the R function NGLVieweR{ NGLVieweR}.

ELISA binding assay

Nunc MaxiSorp 96-well plates were coated with PBS 1% BSA, 1 μg/mL NGAL (SRP6465, Sigma-Aldrich), LL-37 (Proteogenix), or LTF (L4894, Sigma-Aldrich) for 24 h at 4°C. Plates were then washed, and increasing concentrations of LNPEP (ABX654174, LubioScience), PTX3 (ab283455, Abcam), TCN1 (ab236331, Abcam), or OLFM4 (LS-G97738, LSBio) diluted in PBS 1% BSA were added for 1 h at room temperature. Plates were then washed, and 0.5 μg/mL of polyclonal rabbit anti-LNPEP (HPA043642, Sigma Aldrich), anti-PTX3 (SAB4502545, Sigma Aldrich), anti-TCN1 (SAB1411335, Sigma Aldrich), anti–OLFM4 (HPA077718, Sigma Aldrich) diluted in PBS 1% BSA was added for 1 h at room temperature. Plates were then washed, and horseradish peroxidase–conjugated goat anti-rabbit IgG (Thermo Scientific) diluted 1/5,000 in PBS 1% BSA was added to all wells for 30 min at room temperature. Plates were then washed, and TMB substrate was added. Plates were then read at 450 nm with a spectrometer.

Antimicrobial assays

Bacteria (*S. epidermidis* (ATCC 12228)) were cultured at 37°C overnight in brain heart infusion and then subcultured for an additional 3 h to achieve mid–logarithmic phase growth. Bacterial concentrations were measured by spectrophotometry at 620 nm and diluted to a final concentration of 10^5 CFU/mL under low-ionic-strength conditions (10 mM NaCl). To test the antimicrobial activity of recombinant NCPs and its modulation by negatively charged molecules, different concentrations of NGAL (SRP6465, Sigma-Aldrich), LL-37 (Proteogenix), LTF (L4894, Sigma-Aldrich), or LNPEP (ABX654174, LubioScience), PTX3 (ab283455, Abcam), TCN1 (ab236331, Abcam), and OLFM4 (LS-G97738, LSBio) were added to these cultures. To test the antimicrobial activity of endogenous NCPs with live cells, bacterial cultures were added to different amounts of human blood-isolated neutrophils or murine bone-marrow isolated neutrophils in the presence or not of 1 or 5nM OLFM4. To test the antimicrobial activity of endogenous NCPs in the absence of cells, supernantants were harvested from resting or LPS-stimulated (1 μg/mL, LabForce) human or murine neutrophils after a 24-h culture and 5nM OLFM4 was added or not to these supernatants. Bacteria were then added to these supernatants as 10^5 CFU/mL. After 24 h, serial dilutions of bacterial cultures were plated onto blood agar plates. The number of colonies formed after overnight incubation was counted by two independent investigators.

Imaging of NCP binding to bacteria

Bacteria (*S. epidermidis* (ATCC 12228)) were cultured with 1 μM LL-37 in the presence or not of 5nM OLFM4 and plated on poly-L-lysin coated coverslips for 1 h at 37°C. Bacteria were then fixed with 4% PFA for 10 min at room temperature and stained with antibodies for 1 h at room temperature in PBS 1% BSA. Polyclonal rabbit anti-OLFM4 (HPA077718, Sigma Aldrich) and mouse anti-human LL-37 (sc-166770, Santa Cruz Biotechnology) were used at a concentration of 1 μg/mL for 2 h at room temperature followed by secondary goat anti-rabbit IgG (H + L) Cross-Adsorbed -Alexa Fluor 488 (1:500, Thermo Fisher Scientific) and donkey-*anti*-mouse Alexa Fluor 546 (1:500, Invitrogen) antibodies for 1 h at room temperature. After washing, slides were mounted with ProLong Gold antifade mountant with DAPI (Thermo Fisher Scientific) and analyzed on a Zeiss LSM 700 confocal microscope.

DNA condensation assay

DNA condensation assay was performed as previously described[3,12]. Bacterial DNA (1 μg) was incubated with 10 μM of NGAL (SRP6465, Sigma-Aldrich), LL-37 (Proteogenix), or LYZ (Sigma-Aldrich) for 15 min at room temperature in TE buffer (10 μM Tris-Cl, pH 7.4 and 1 μM EDTA) to allow complex formation. Complexes were then stained with PicoGreen (Quant-iT PicoGreen double-stranded DNA kit, Invitrogen) according to the manufacturer's standard protocol. Samples were excited at 480 nm, and the emission intensity was measured at 520 nm. The sudden decrease in DNA staining occurring because of DNA-NCP complex formation is indicative of DNA condensation and results from both dye exclusion as well as quenching of the fluorescence.

Isolation and stimulation of neutrophils and pDCs

Human Peripheral Blood Mononuclear Cells (PBMCs) were obtained from healthy donors' buffy coats (Interregional Blood Transfusion SRC Ltd) by centrifugation on Ficoll gradient (GE Healthcare). Neutrophils were isolated using the EasySep Direct Human Neutrophils Isolation Kit and pDC were isolated using the EasySep Human Plasmacytoid DC Isolation Kit following manufacturer's instructions (StemCell). For murine neutrophils, femur and tibia bones from WT and Olfm4−/− male and female mice were harvested and the bone marrow was flushed out with PBS 2% FBS 2mM EDTA. Neutrophils were then isolated using the EasySep Mouse Neutrophil Enrichment Kit following manufacturer's instructions (StemCell). Cell purity was assessed by flow cytometry using CD16-PE (1:50, BD) and CD66b-APC (1:100, eBioscience) staining of human neutrophils (purity> 95%), CD123-PerCP.Cy5.5 (1:200, BioLegend), BDCA4-APC, and BDCA2-PE (1:50, Miletnyi) staining of human pDCs (purity>95%), and CD11b-PE (1:500, BioLegend), Ly6G-PE (1:1000, BD Bioscience), and Ly6C- PerCP.Cy5.5 (1:500, eBioscience) staining of murine neutrophils (purity>75%).

For cell stimulation, neutrophils and pDCs were plated at 10^6 cells/ml and stimulated with bacterial DNA isolated from *S. epidermidis* (ATCC 12228) (1 μg/mL) complexed or not with LL-37 (50 μg/mL, Proteogenix) in the presence of different concentrations of human (LS-G97738) or murine (LS-G11718) OLFM4 (LSBio). As control, neutrophils were stimulated with LPS (1 μg/mL, LabForce). For all experiments, cell-free supernatants were collected after overnight stimulation to measure human type I IFN by ELISA (Mabtech), human IL-6, human CXCL8, and human TNF by CBA (BD biosciences), or murine TNF, murine IL-6, and murine IFNγ by LEGENDplex Mouse Inflammation Panel (BioLegend).

Gene expression profiling

Excised tissue from murine injured skin was immediately snap-frozen in liquid nitrogen and stored at −80°C until RNA was isolated. RNA was isolated using the TRIzol (1mL)/chloroform (200μl) method and a tissue homogenizer (Thermo Fisher Scientific). QC was run on a Fragment analyzer (Agilent) to select RNAs with A260/A280 value of ≥1.7, RNA integrity ~10 and a DV300 > 50%. The mRNA expression of 785 targets was then analyzed with the nCounter murine Host Response panel (Nanostring Technologies) on the nCounter platform (Nanostring Technologies) using 100 ng of RNA per skin sample. Normalization and analysis were then performed using the nSolver 4.0 software (Nanostring Technologies).

QUANTIFICATION AND STATISTICAL ANALYSIS

Statistical analyses are described in each figure legend. Normal distribution of data was tested using Shapiro-Wilk test. When normality tests were inconclusive due to small sample sizes, ANOVA was used as it has more power than its non-parametric counterpart. For experiments combining several groups, two-sided one-way or two-way ANOVA tests were used. Significant differences between groups were determined by post-hoc Tukey's multiple comparisons tests or Sidak's multiple comparisons test, unless specified otherwise, using GraphPad Prism 9.0 software. $p > 0.05$ was considered nonsignificant.